

# Gd<sub>2</sub>O<sub>3</sub>:Eu<sup>3+</sup> phosphor particles processed through aerosol route

M.E. Rabanal<sup>a,\*</sup>, C. Moral<sup>a</sup>, J.M. Torralba<sup>a</sup>, L. Mancic<sup>b</sup>, O. Milosevic<sup>b</sup>

<sup>a</sup> University Carlos III, Avda. Universidad 30, 28911 Leganes, Madrid, Spain

<sup>b</sup> Institute of Technical Sciences of SASA, K. Mihajlova 35/IV, 11000 Belgrade, Serbia and Montenegro

Available online 2 April 2005

## Abstract

In this work, the influence of the Eu<sup>3+</sup> luminescence center concentration on the structural, morphological and spectroscopic properties of powders obtained by an aerosol method was studied. In the method, gadolinium and europium nitrate solutions were ultrasonically aerosolised and fed into a high-temperature (up to 1200 °C) tubular flow reactor to control the aerosol decomposition. During decomposition, the aerosol droplets undergo evaporation/drying, precipitation and thermolysis in a single-step continuous process. Spherical, solid, agglomerate-free, submicron-sized particles with the crystallite sizes below 20 nm have been obtained. In order to control the particle crystal structure and to establish the conditions for the stabilization of the low-temperature gadolinia cubic phase, process parameters such as synthesis temperature, droplet/particle residence time and annealing temperatures were varied. The particle morphology, phase and chemical structure were studied by X-ray diffraction (XRD), scanning electron microscopy (SEM) and EDS. Structural changes (crystallite size and microstrains) after powders thermal treatment were carried out using the Koalariet-XFit program as the profile-matching tool.

The results obtained and the mechanisms for ultrafine phosphor particle generation are discussed in terms of precursor chemistry, process parameters and luminescence properties.

© 2005 Elsevier Ltd. All rights reserved.

**Keywords:** Powders-gas phase reaction; X-ray methods; Optical properties; Gd<sub>2</sub>O<sub>3</sub>:Eu phosphor particles

## 1. Introduction

Advanced phosphor materials processing requires the control of ultrafine powder properties. Light emission efficiency, caused by the interaction between atomic states associated with the luminescence center and the host lattice material,<sup>1</sup> is primarily affected by the homogeneity in dispersion of activator ions. Additionally, superior luminescence properties have been attained in phosphor particles having a spherical morphology, a submicrometer size and a narrow particle size distribution.<sup>2</sup> Spray pyrolysis is one of the basic aerosol routes which can provide such structural properties in a powder. It is relatively low cost, simple to manipulate and adaptable to large-scale production. In this process, a precursor solution is dispersed as an aerosol and is carried into a flow reactor by means of a pressure differential. Under the correct conditions, the precursor salts react to form the desired

compounds inside the furnace. Gadolinium oxide has been extensively used in a variety of applications.<sup>3</sup> When it is activated by rare earth elements (ie. Eu<sup>3+</sup> or Nd<sup>3+</sup>), it becomes an effective crystal phosphor, showing cathodo-luminescence and laser action.<sup>4</sup> In a continuation of our previous studies on Gd<sub>2</sub>O<sub>3</sub>:Eu red phosphor material synthesis through spray pyrolysis,<sup>5</sup> the goal of this paper is to investigate the influence of the Eu<sup>3+</sup> luminescence center concentration on the structural, morphological and spectroscopic properties of powders obtained under different temperature regimes, residence times and annealing temperatures.

## 2. Experimental

The spray pyrolysis experimental set-up consists of an ultrasonic nebulizer operated at 1.7 MHz, a quartz tube located inside a cylindrical furnace and particle collector (Fig. 1). The fine drops of precursor solutions were carried out by the air-flow regulated with a flow controller. The details of the estab-

\* Corresponding author. Tel.: +34 91 624 99 16.

E-mail address: [eugenia@ing.uc3m.es](mailto:eugenia@ing.uc3m.es) (M.E. Rabanal).



Fig. 1. Schema of the spray pyrolysis reactor.

lished synthesis conditions and the calculated droplet/particle residence times are presented in Table 1. Two precursor solutions having the same overall concentration of nitrates ( $0.1 \text{ mol/dm}^3$ ) were prepared by dissolving the appropriate amounts of  $\text{Gd}(\text{NO}_3)_3 \cdot 6\text{H}_2\text{O}$  and  $\text{Eu}(\text{NO}_3)_3 \cdot 6\text{H}_2\text{O}$  in order to obtain either 0.95:0.05 or 0.90:0.10 Gd:Eu molar ratio (as-prepared samples are denoted S05 and S1, respectively). After synthesis, the powders were annealed isothermally at  $800\text{--}1200^\circ\text{C}$  in a chamber furnace in air. The analysis were performed at the 500 mg powder batches.

The crystal structure of the as-prepared and thermally treated powders was analysed by X-ray diffraction (XRD) collected in an automatic X'Pert Philips diffractometer, and using a Cu  $K\alpha$  source. Data were collected in the  $2\theta$  ranges from  $15^\circ$  to  $60^\circ$  in step-scanning mode with a step size of  $0.02^\circ$  and a counting time of 5–18 s per step. Structural refinements were carried out using the Koalariet-Xfit<sup>6</sup> Rietveld program. Compositional homogeneity and particle morphology were analysed by scanning electron microscopy (SEM, Hitachi S-800; SEM S-4500), and energy dispersive X-ray spectroscopy (EDX prime). Luminescence properties were measured in the range 500–700 nm with a sharp excitation spectra excitation wavelength of Ar laser (10 mW) at 366 nm.

### 3. Results and discussion

SEM photographs of powder samples S05 and S1 are shown in Fig. 2. They implied formation of individual parti-

cles with spherical shape and solid morphology. The smooth particle surface is characteristic of as-prepared powders, while a rough surface is detectable after annealing due to the further promotion of the crystallization process. A narrow particle size distribution was found for all powder samples. The mean particle size in the as-prepared powder (sample S05) was determined to be 800 nm. Comparing the particle sizes derived from the SEM photomicrographs, it can be seen that particle size slightly decrease during thermal treatments as a consequence of additional densification, but the morphology and shape of the particles remain the same.

According to the EDS area analysis for serial S05, the concentration of europium in the as-prepared powdered sample for particle of diameter  $1.64 \mu\text{m}$  is 3.95 at.%. After annealing, europium ion concentration is determined as to be 2.99 at.% for particle having the diameter of  $1.1 \mu\text{m}$ . EDS spot analysis performed in randomly chosen particles in samples from serial S1 indicate a slightly variable activator ion content in different sized particles, however, for all samples, the concentration ranged from 2.1 to 4.4 at.%.

XRD phase analyses implied the presence of the cubic  $\text{Gd}_2\text{O}_3$  phase (file card 43-1014) in all samples. In addition to  $\text{Gd}_2\text{O}_3$ , another cubic phase is evident in the as-prepared powders (12 wt.% in S1). This phase is structurally similar to the  $\text{Gd}_2\text{Te}_6\text{O}_{15}$  (SSI) (file card 37-1400) and corresponds to the intermediate solid solution with a disordered  $\text{CaF}_2$  type structure in which  $\text{Eu}^{2+}$  ions can exchange  $\text{Te}^{4+}$  or  $\text{Eu}^{3+}$  ions can substitute  $\text{Gd}^{3+}$ . Extensive ions exchange is very possible because of the close ionic radius match for octahedral coordinations ( $\text{Eu}^{2+}$ : 0.112 nm;  $\text{Te}^{4+}$ : 0.111 nm.;  $\text{Eu}^{3+}$ : 0.095 nm;  $\text{Gd}^{3+}$ : 0.094 nm). It seems that this intermediate phase evolution is additionally influenced by the synthesis conditions that enable partially  $\text{Eu}^{3+}$  ion reduction to  $\text{Eu}^{2+}$  due to the oxygen depletion at the particle surface caused by the high concentration of adsorbed nitrogen. The presence of nitrogen is evident in the EDS analysis of the as-prepared particles. The corresponding peak ratio of SSI (1 1 1) ( $2\theta \approx 27.5^\circ$ )-to-cubic gadolinium oxide (2 2 2) ( $2\theta \approx 28.5^\circ$ )-phase,  $I_{\text{SSI}(111)}/I_{(222)}$ , is 4.7 and 0.33, for as-prepared powder samples S05 and S1, respectively. This phase disappeared after annealing above  $400^\circ\text{C}$ .<sup>5</sup> The presence of cubic gadolinia is evident in both sample serials after annealing. A typical XRD pattern after fit-

Table 1  
Synthesis conditions and structural characteristic of as-prepared and annealed samples

Sample	Airflow rate ( $\text{dm}^3/\text{min}$ )	Aerosol flow ( $\text{ml}/\text{min}$ )	Residence time <sup>a</sup> in furnace/on $T_{\text{max}}$ (s)	Synthesis or annealing temperature ( $^\circ\text{C}$ ) and time (h)	Crystallite size (nm) and microstrain (%)	Crystal cell parameter ( $\text{Å}$ )
S05	1.5	0.38	34/16	200/600/900	–	–
S05-1				800; 24	27.9; 0.079	10.8214
S05-2				1200; 8	49.5; 0.001	10.8293
S1	1.5	0.28	84/31	700	16.2; 1.183	10.8040
S1-1				800; 12	60.7; 0.233	10.8212
S1-2				900; 12	54.4; 0.214	10.8244
S1-3				1000; 12	–	–

<sup>a</sup> Calculated from the airflow rates and the geometry of the reactors.

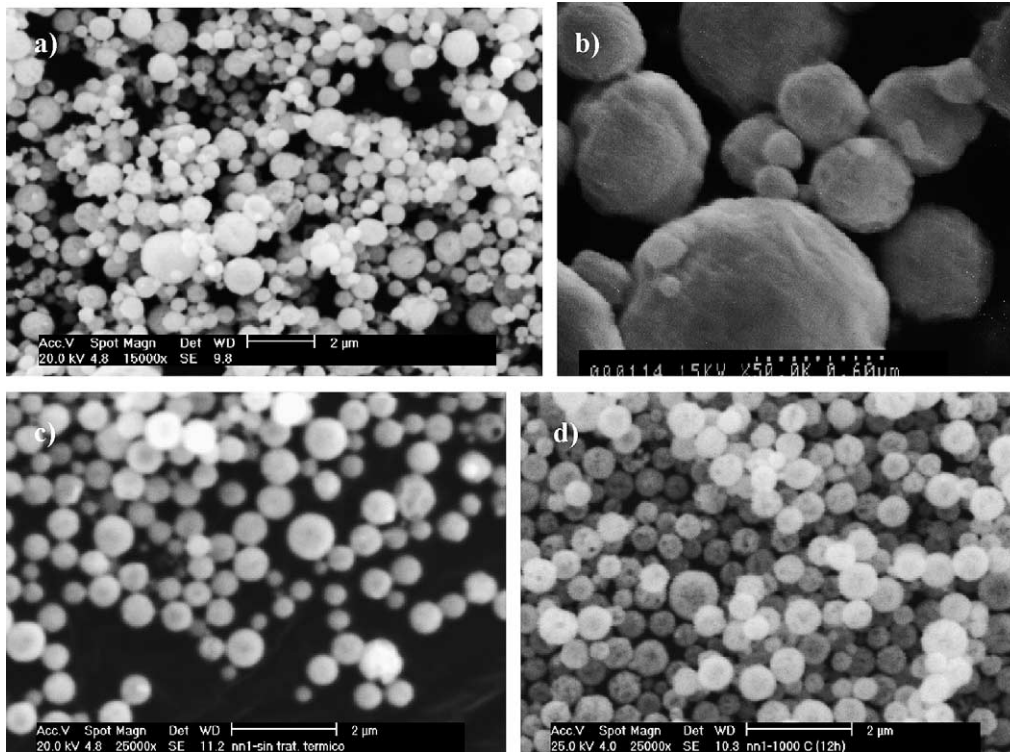


Fig. 2. SEM photomicrographs of  $Gd_2O_3:Eu$  particles prepared through spray pyrolysis: (a) S05-1; (b) S05-2; (c) S1; and (d) S1-3.

ting, together with the resulting difference curve is presented at Fig. 3a. The estimated values of the cell parameters for the cubic gadolinium oxide phase, presented in Table 1, imply the tendency of the crystal cell to increase with an increase in the thermal treatment temperature.

The structural changes expressed through average crystallite size and lattice microstrains, presented in Table 1, imply a gradual increase in crystallinity as well as a decrease in microstrains with increasing annealing temperature. The main feature of the as-prepared particles is the presence of the small primary crystallites. Promotion of crystallite growth is evident in thermally treated samples. Particle surface rough-

ness, apparent in Fig. 2b, results from the thermally induced crystallite growth, collisions and aggregation into clusters.

The relationship between the crystal cell parameter, the thermal treatment temperature and the europium content, determined as the mean value of EDS spot analysis data obtained in randomly chosen particles, is presented at Fig. 3b. The gradual increase of crystal cell with both temperature and Eu at.% could be associated with the  $Eu^{3+}$  ion incorporation into the gadolinium oxide matrix, since it is a thermally induced diffusion process.

The substitution of  $Gd^{3+}$  lattice sites with europium ions in gadolinium oxide matrices is additionally confirmed in the

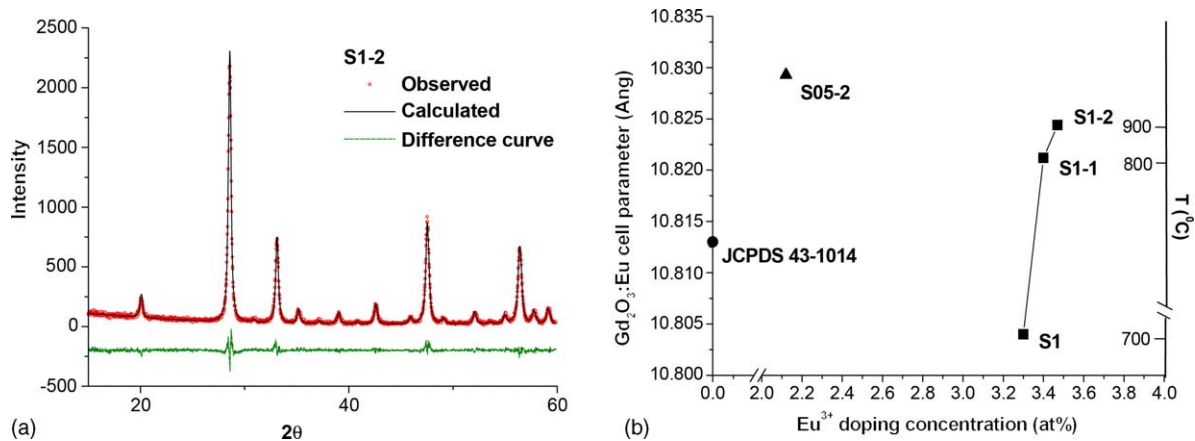


Fig. 3. Typical XRD pattern of  $Gd_2O_3:Eu$  powder prepared through spray pyrolysis after additional thermal treatment (a);  $Gd_2O_3:Eu$  cell parameter vs. determined  $Eu^{3+}$  ion doping concentration (EDS) and temperature (b). Line is drawn as a guide for the eye.

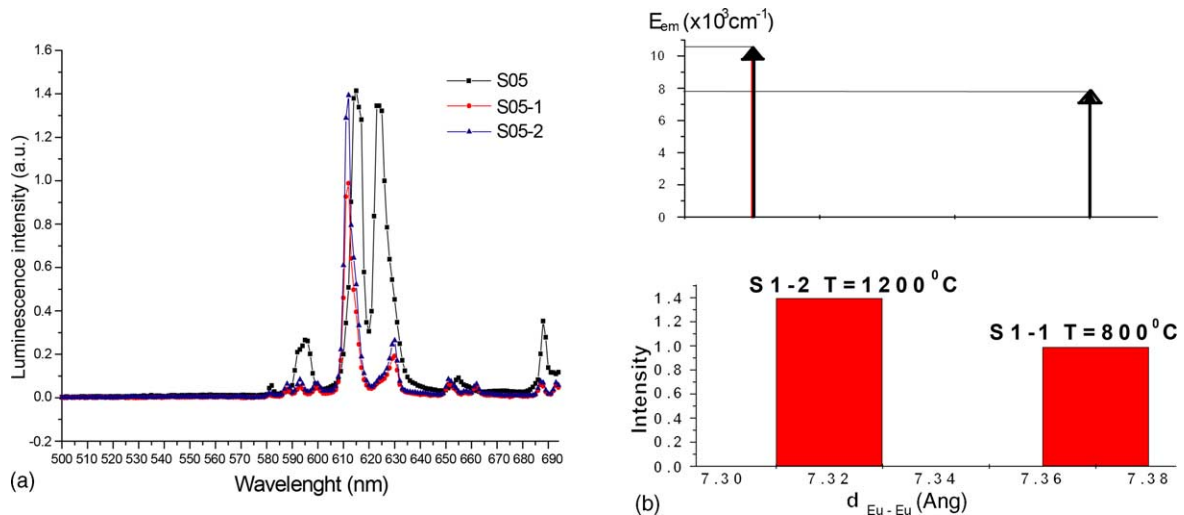


Fig. 4. Photoluminescence intensities of  $\text{Gd}_2\text{O}_3:\text{Eu}$  particles (a); Emission energy as a function of the calculated Eu–Eu distance for determined  $\text{Eu}^{3+}$  ion doping concentration (EDS) (b).

serial S05 powder samples by red emission and by the appearance of two dominant peaks at 615 and 624 nm (Fig. 4a). The emission band at 624 nm is probably related to the intermediate solid solution phase (SSI) as revealed by XRD and by previous results.<sup>6</sup> The sharp emission band peaking at 612 nm has the highest intensity for sample S05-2. This emission line corresponds to the  $^5\text{D}_0 \rightarrow ^7\text{F}_2$   $\text{Eu}^{3+}$  transition for the  $\text{C}_2$  crystallographic site in the gadolinium oxide matrix.<sup>4</sup>

In Fig. 4b, the emission energy is presented as a function of the calculated Eu–Eu distance for different  $\text{Eu}^{3+}$  ion doping concentrations and is determined as follows<sup>7</sup>:

$$d_{\text{Ce}-\text{Ce}} = 2 \left[ \frac{V_{\text{Eu}}}{4/3\pi} \right]^{1/3} \quad (1)$$

where

$$V_{\text{Eu}} = \frac{1}{N_a} \frac{V_m}{X_{\text{Eu}}}, \quad (2)$$

where  $V_m$  is a molar volume calculated from the weighed-out composition,  $N_a$  is Avogadro number and  $X_{\text{Eu}}$  is the  $\text{Eu}^{3+}$  concentration (determined as the mean value of corresponding EDS spot analysis). Fig. 4b confirms the results reported for other systems,<sup>7,8</sup> where a higher activator ion content reduces the distance between luminescent centers and increase the emission intensity.

#### 4. Conclusions

Submicron-sized and exceptionally well structurally and morphologically defined nanophased  $\text{Gd}_2\text{O}_3:\text{Eu}$  phosphor particles were prepared by a spray pyrolysis method. All produced particles were spherical and nonagglomerated with a narrow particle size distribution. It was shown that unifor-

mity of the phase content influences luminescence causing the appearance of two dominant peaks at 615 and 625 nm for as-prepared powder. A sharp emission band at 612 nm associated with a pure cubic gadolinium structure formed after additional thermal treatment. The structural changes, together with the retention of the desired morphology, results in enhanced luminescence properties for the thermally treated powders. These characteristics, along with the high reactivity of particles produced through spray pyrolysis, make them suitable for obtaining good packing densities in practical display applications.

#### Acknowledgements

This research was financially supported through the NEDO International Joint Research Grant Program 01MB7: “Wetability of solid by liquid at high temperatures”, as well as Republic of Serbia Science Foundation grant no. 1832.

#### References

- Kim, E. J., Kang, Y. C., Park, H. D. and Ryu, S. K., UV and VUV characteristics of  $(\text{YGd})_2\text{O}_3:\text{Eu}$  phosphor particles prepared by spray pyrolysis from polymeric precursors. *Mater. Res. Bull.*, 2002, **38**(3), 515–524.
- Zhai, Y. Q., Yao, Z. H., Qiu, M. D., Liu, B. S. and Dai, X. L., Synthesis and luminescent properties of  $\text{Gd}_2\text{O}_3:\text{Eu}$  nanocrystalline using EDTA complexing sol–gel process. *Indian J. Chem. A*, 2004, **43**(1), 71–75.
- Brenier, A. and Boulon, G., Laser heated pedestal growth and spectroscopic investigations of  $\text{Nd}^{3+}$ -doped  $\text{Gd}_2\text{O}_3$  single crystal fibres. *J. Lumin.*, 1999, **82**, 285–289.
- Buijs, M., Meyernik, A. and Blasse, G., Energy transfer between  $\text{Eu}^{3+}$  ions in a lattice with two different crystallographic sites:  $\text{Y}_2\text{O}_3:\text{Eu}^{3+}$ ,  $\text{Gd}_2\text{O}_3:\text{Eu}^{3+}$  and  $\text{Eu}_2\text{O}_3$ . *J. Lumin.*, 1987, **37**, 9–20.

5. Milosevic, O., Mancic, L., Jordovic, B., Maric, R., Ohara, S. and Fukui, T., Processing of  $Gd_2O_3:Eu$  phosphor particles through aerosol route. *J. Mater. Process. Technol.*, 2003, **143–144**, 501–505.
6. Cheary, R. W. and Coelho, A. A., *Programs XFIT and FOURYA*. CCP14 Powder diffraction Library-Daresbury Laboratory, Warrington, UK, 1996.
7. de Graaf, G., Hintzen, H. T. and de With, G., The influence of the composition on the luminescence of Ce(III)–Ln–Si–Al–O–N glass (Ln = Sc, Y, La, Gd). *J. Lumin.*, 2003, **104**, 131–136.
8. del Rosario, G., Ohara, S., Mancic, L. and Milosevic, Characterization of YAG:Ce powders thermal treated at different temperatures, *Appl. Surf. Sci.*, 2004, **238**(1–4), 469–474.